Available online at www.sciencedirect.com

ScienceDirect

IFAC PapersOnline CONFERENCE PAPER ARCHIVE

IFAC PapersOnLine 51-34 (2019) 372–377

The influence of different types of inceptors and their characteristics on the pilot-aircraft system

A.V. Efremov, V.V. Aleksandrov, E.V. Efremov, M.V. Vukolov

Moscow aviation Institute, Moscow, Russia (e-mail: pvl@mai.ru)

Abstract: The manipulator is one of the task variables of pilot-vehicle system. The influence of its type (side stick and central stick), some of inceptor's parameters (stiffness, damping) were studied in the paper. For each variable the difference between the displacement sensing control and force sensing control were investigated as well. Each investigation was carried out on the fixed based simulator when the operator executed the pitch control task with the different dynamic configurations. The experiments in the lateral channel were carried out mainly to expose the difference between the pilot actions in longitudinal and lateral channels. The pilot structural model was modified with goal to extend its potentialities for the prediction of influence of the feel system parameters on pilot behavior.

Keywords: pilot-aircraft system; pilot control response characteristics; simulation; flying qualities; flight control system.

1. INTRODUCTION

The main part of flying qualities investigations are carried out with the feel system characteristics (force gradient F_δ, force damping $F_{\dot\delta}$ and others) and controlled element gain coefficient (control sensitivity K_C) which is selected according to the pilot opinion. The analysis of the published papers [1-8] demonstrates the influence of type of inceptor (wheel, side or central stick), feel system characteristics and controlled element gain coefficient on pilot-aircraft system parameters and flight safety, in particular, on pilot-induced oscillations, roll rachet events and biodynamic pilot-aircraft interaction. They influence also on pilot ratings, on different pilot-aircraft characteristics (resonant peak of the closed loop system, crossover frequency, task performance, etc.). At the same time there is no regular technique for the optimization of the feel system characteristics or controlled element gain coefficient based on the mathematical modeling of pilot-aircraft system. In case when the inceptor and dynamics of the designed aircraft are similar to the prototype, the prototype's characteristics are used in preliminary design and then they are checked in ground based and in-flight investigations. The appearance of the new type of manipulators – active side stick, force sensing control (FSC) type of manipulator, requires the revision of the previous recommendations, and intensive wide experimental research. The results discussed in the paper were obtained in the detailed investigation carried out with goal to extend the knowledge of influence of inceptors's characteristics (stiffness, damping), its type (central stick and side stick, force sensing and displacement sensing control (DSC) inceptors) on pilot-aircraft system characteristics. It was done to expose the main regularities of pilot-inceptor different vehicle for the dynamics. The authors consider all these results as the basis for the development of the technique basing on pilot-aircraft system analysis necessary for the following use in the optimization of the feel system characteristics and control sensitivity for selection of inceptor's type. The technique for optimization of the controlled element gain coefficient is based on minimization of the cost function and the use of pilot structural model is considered in [9]. The last part of the paper is dedicated to the modification of this structural model and its application for prediction of the influence of the stick stiffness and type of manipulator on pilot-aircraft system.

2. THE EXPERIMENTAL INVESTIGATIONS

The dynamics of the feel system can be described by the following equation:

$$m\ddot{x} + F^{\dot{x}}\dot{x} + F^{x}x = \Delta F,$$

or the corresponding transfer function:

$$\frac{x(s)}{F(s)} = \frac{\frac{1}{m}}{s^2 + \frac{F^{\dot{x}}}{m}s + \frac{F^{x}}{m}} = \frac{Y_m}{s^2 + 2\xi_{fs}\omega_{fs}s + \omega_{fs}^2}, \quad (1)$$

where m – mass of inceptor, $F^{\dot{x}}$ - it's damping, F^{x} - stiffness, x – inceptor displacement, ΔF - force applied by pilot.

In case of the DSC inceptor, whose output is the displacement, we can expect a higher phase lag in comparison with the FSC inceptor, whose output is the force ΔF. The results of experiments given in [2-3] confirm this conclusion for the lateral tracking task. The

10.1016/j.ifacol.2019.01.013

current paper is dedicated mainly to the investigation of the pitch control tracking task with different dynamic configurations given in the table 1.

Table 1 The configurations investigated in longitudinal channel

W_C	$\frac{K_C}{s}$	$\frac{K_C}{s(s+1)}$	HP 2.1	HP 5.10

The dynamic configurations HP 2.1, HP 5.10 were taken from Have PIO data base [10]. The parameters of their transfer functions between the pitch angle (θ) and inceptor input (δ_e) are different and correspond to the different flying qualities level. Configuration HP 2.1 belongs to the first flying qualities (FQ) level and configuration HP 5.10 corresponds to the third FQ level.

The roll tracking task was investigated for a limited number of configurations (table 2) to expose mainly the difference in pilot actions in longitudinal and lateral channels.

Table 2 The configurations investigated in lateral channel

W_C	$\frac{K_C}{s}$	$\frac{K_C}{s(0.25s+1)}$	$\frac{K_C}{s(0.25s+1)}e^{-0.07s}$

The experiments were carried out with the central and side sticks. The variable values of stiffness F^x and relative damping for the central stick are given in table 3.

Table 3 Feel system parameters

	1	2	3
$F^x, N/sm$	1	10	30
ξ_{fs}	0.05	0.5	1.5

As for the side stick, the experiments were carried out in the longitudinal channel for two values of the stiffness (F^x): $5\,N/sm$ *and* $15\,N/sm$. In the lateral channel the side stick had two values of the stiffness (F^x): $4.2\,N/sm$ *and* $10\,N/sm$. The sufficient accent in investigation was made on exposition of the difference between the FSC and DSC type of control signal transmition to the flight control system for the both inceptors. All parameters of feel system were simulated with help of MOOG feel system (fig. 1). The experiments were carried out on MAI moving based simulator (fig. 2), equipped with computer generated visual system and MOOG feel system in all control channels.

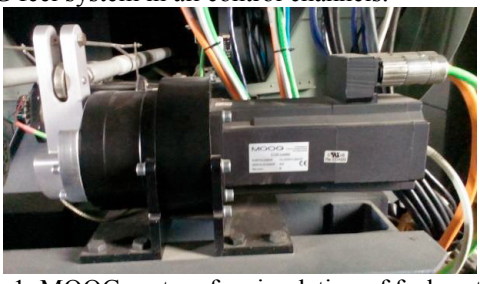

Fig. 1. MOOG system for simulation of feel system parameters

Fig. 2. MAI ground based simulator

Two operators which included a pilot participated in different experimental investigations.

The piloting tasks were the single loop tracking tasks in longitudinal or lateral channels. The input signal in these tasks was the sum of the same set of harmonics in the frequency range 0.26 – 15.7 rad/sec with the different variances. The frequencies of these harmonics are shown on fig. 3, 4, 6, 7, 8, 12, 13 as the point (○····○) for DSC or (✦····✦) for FSC type of stick. The variance σ_i^2 in the pitch tracking task was equal to 4 sm^2 and 200 deg^2 in lateral channel.

The results of the experimental investigations were used for the following comparison with results of the mathematical modeling pilot-aircraft system.

The experiments carried out with the side stick for configurations HP 2.1 (I level of flying qualities) and HP 5.10 (III level of flying qualities) demonstrated that in case of FSC side stick the pilot phase delay was considerably smaller. The phase delay was characterized by parameter $\Delta\varphi\big|_{\omega=10\ rad/sec} = \varphi_{FSC} - \varphi_{DSC}$.

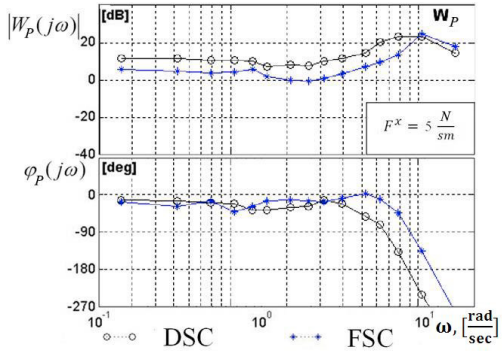

Fig. 3. Pilot describing function for conf. HP 2.1

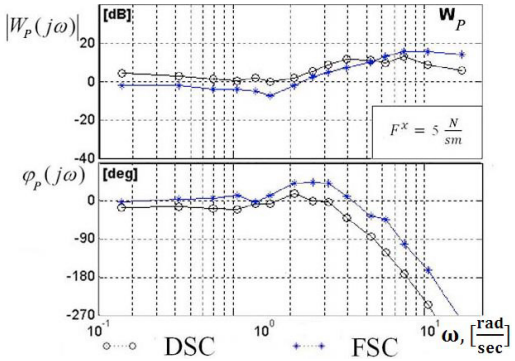

Fig. 4. Pilot describing function for conf. HP 5.10

$\Delta\varphi|_{\omega=10\ rad/sec} = \varphi_{FSC} - \varphi_{DSC}$, where φ_{FSC} and φ_{DSC} are the pilot phase frequency response characteristics for the FSC and DSC inceptors correspondingly. It was equal to 106 deg in experiments with configuration HP 2.1 and stiffness $F^X = 5\ N/sm$, which is equivalent to the time delay $\Delta\tau \cong 0{,}18\,sec$. In experiments with higher stiffness, $\Delta\varphi|_{\omega=10\ rad/sec}$ decreases up to 40 deg at the same frequency (fig. 3).

Except that, the experiments with FSC inceptor were accompanied by the decrease of variance of error σ_e^2 by 1,5 times and the increase of crossover frequency ω_C up to 30 %.

As for configuration HP5.10 the influence of type of inceptor (DSC or FSC) on phase delay parameter $\Delta\varphi|_{\omega=10\ rad/s}$ is smaller and reaches 80 deg only (fig. 4).

The similar effects were observed with the central stick. They demonstrated more sufficient and specific influence of spring stiffness on the results. For example the dependence of variance σ_e^2 as a function of F^x has the minimum (see fig. 5).

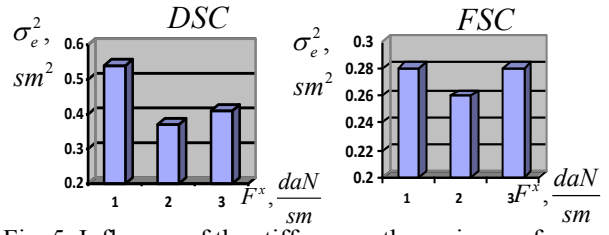

Fig. 5. Influence of the stiffness on the variance of error

In case of the central stick, the difference between pilot phase frequency characteristics in experiments with FSC and DSC type of inceptors was exposed too. The values of parameter $\Delta\varphi|_{\omega=10\ rad/sec}$ lies in the range 102 deg (conf. $\frac{K_C}{s(s+1)}$) ÷ 74.4 deg (conf. HP 5.10).

The influence of the central stick stiffness on pilot-aircraft system characteristics exposed in experiments with the different configurations are given in the tables 4–6.

Table 4 The pilot-aircraft system characteristics (conf. $W_C = \frac{K_C}{s(s+1)}$)

Type of stick	σ_e^2, sm^2			$\omega_C, rad/sec$		
$F^x, \frac{N}{sm}$	1	10	30	1	10	30
DSC	0.96	0.69	0.76	1.31	1.21	1.16
FSC	0.38	0.34	0.62	2.59	2.56	1.66

Type of stick	$\omega_{BW}, rad/sec$			$\Delta\varphi|_{\omega=10\ rad/sec}$, deg		
$F^x, \frac{N}{sm}$	1	10	30	1	10	30
DSC	1.65	1.42	1.47	101.9	27.6	23.1
FSC	2.9	2.83	1.79			

Table 5 The pilot-aircraft system characteristics (conf. HP 2.1)

Type of stick	σ_e^2, sm^2			$\omega_C, rad/sec$		
$F^x, \frac{N}{sm}$	1	10	30	1	10	30
DSC	0.54	0.37	0.41	2.25	3	2.87
FSC	0.28	0.26	0.28	3	3.09	2.5

Type of stick	$\omega_{BW}, rad/sec$			$\Delta\varphi|_{\omega=10\ rad/sec}$, deg		
$F^x, \frac{N}{sm}$	1	10	30	1	10	30
DSC	3.31	3.28	3.64	81	33	13.9
FSC	3.43	3.58	3.63			

Table 6 The pilot-aircraft system characteristics (conf. HP 5.10)

Type of stick	σ_e^2, sm^2			$\omega_C, rad/sec$		
$F^x, \frac{N}{sm}$	1	10	30	1	10	30
DSC	1.24	1.07	1.18	1.54	1.51	0.98
FSC	1.014	0.97	1.11	0.99	1.44	0.72

Type of stick	$\omega_{BW}, rad/sec$			$\Delta\varphi|_{\omega=10\ rad/sec}$, deg		
$F^x, \frac{N}{sm}$	1	10	30	1	10	30
DSC	1.76	1.80	1.5	74.4	20.8	0.4
FSC	2.46	1.67	1.48			

Here, ω_{BW} is the bandwidth frequency of the closed-loop system.

The comparison of the accuracy achieved for the central and side sticks demonstrated higher crossover frequency and the smaller variance σ_e^2 in experiments with the side stick specially for the FSC type of inceptor (by 1.4 times for configuration HP-21).

The influence of damping was investigated for the central stick. The results of this investigation are given in the table 7 for the configuration HP 2.1. They demonstrate that the considerable increase of the damping causes the

increase in the variance of error, the decrease of the crossover ω_C and the bandwidth ω_{BW} frequencies and the increase in the phase delay parameter $\Delta\varphi|_{\omega=10\ rad/sec}$. The same tendencies were exposed for the other dynamic configurations too.

Table 7 The pilot-aircraft system characteristics (conf. HP 2.1)

Type of stick	σ_e^2, sm^2			$\omega_C, rad/sec$		
ξ_{fs}	0.05	0.5	1.5	0.05	0.5	1.5
DSC	0.53	0.53	0.82	2.15	2.12	1.5
FSC	0.39	0.51	0.52	2.32	1.75	2.09
Type of stick	$\omega_{BW}, rad/sec$			$\Delta\varphi\|_{\omega=10\ rad/sec}$, deg		
ξ_{fs}	0.05	0.5	1.5	0.05	0.5	1.5
DSC	2.75	2.58	2.35	71	55	140
FSC	3	2.56	2.64			

A number of experiments were carried out separately in single loop pitch and roll tracking tasks with the same control element dynamics $W_c = \frac{K}{s}$ or $W_C = \frac{K}{s(0.25s+1)}$. In case when the two degree of freedom side stick was used the results demonstrated the difference between pilot describing functions in these channels. This is due to of the different joints that realize the hand movements. In the longitudinal channel the motion is realized basically by translational movement of hand bent in elbow joint. In the lateral channel, the displacement of the side stick is realized by the rotation of the hand, in the hand joint. In the case when pilot used the central stick, his command input in lateral channel is realized by the translational lateral displacement of the hand. The influence of these different ways of the stick displacement on pilot frequency response characterisrics are given in fig. 6-7. It is seen that in case $W_c = \frac{K}{s}$ the pilot phase characteristics are close.

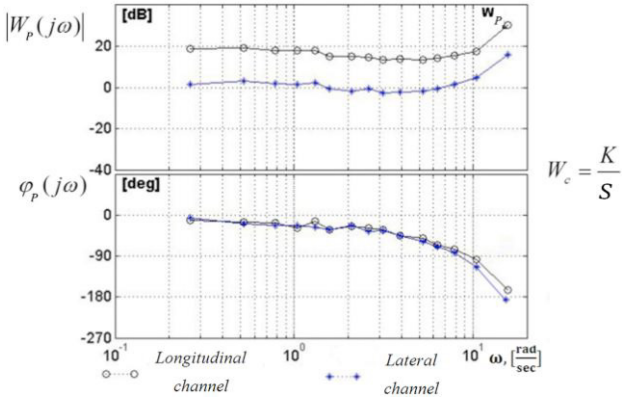

Fig. 6. Pilot describing function for the longitudinal and lateral channels

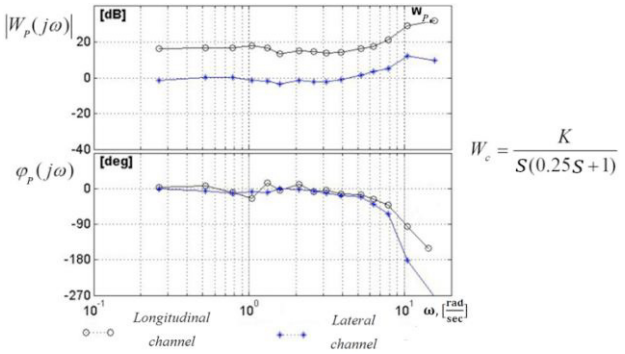

Fig. 7. Pilot describing function for the longitudinal and lateral channels

At the frequency $\omega = 10$ rad/sec the difference is 16 deg. For controlled element dynamics $W_C = \frac{K}{s(0.25s+1)}$ the difference increases up to 90 deg. It means that the time delay (τ) is higher in lateral channel then in comparison with longitudinal channel up to 0.03 sec in case $W_c = \frac{K}{s}$ and up to 0.15 sec in case $W_C = \frac{K}{s(0.25s+1)}$. Thus the use of the side stick requiring the rotation of the hand joint in lateral channel is accompanied by the increase of the time delay in comparison with the case when the translational type of hand actions are required. In case when the central stick is used for the tracking tasks in lateral or longitudinal channel there are no such effects. Such peculiarity is accompanied by the increase of the relative error $\frac{\sigma_e^2}{\sigma_i^2}$ up to 40 % in the lateral channel in comparison with the longitudinal channel during the experiments with the side stick. The roll tracking task experiments demonstrated the same effect of FSC inceptor type of the stick – the decrease of pilot phase delay in comparison with the DSC inceptor (fig. 8).

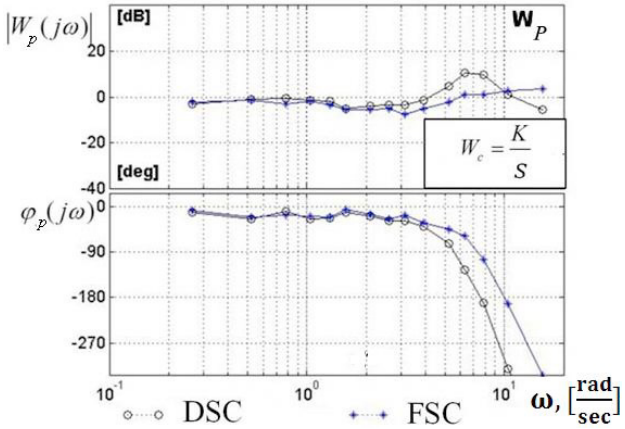

Fig. 8. The influence of DSC and FSC on $W_P(j\omega)$ in lateral channel

These values are more sufficient in comparison with the experiments in longitudinal channel and depend on the spring stiffness (fig. 9).

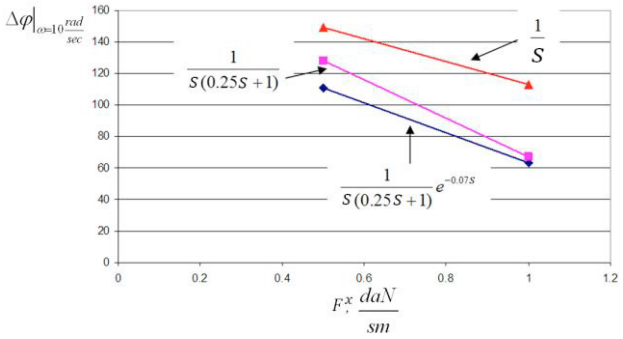

Fig. 9. The influence of the spring stiffness in lateral channel

The use of FSC inceptor allows to achieve the reduction in variance of error. For the controlled element dynamics $W_c = \frac{K}{s(0.25s+1)}$ or $W_c = \frac{K}{s(0.25s+1)}e^{-0.07s}$ the variance σ_e^2 decreases by 1.5÷1.6 times in comparison with DSC inceptor.

2. THE MATHEMATICAL MODELING OF PILOT-AIRCRAFT SYSTEM

The structural model of pilot behavior developed by R. Hess [11] is used widely for solution of different manual control tasks. It was modified several times, and one of the last modification developed by the authors [9] allows to extend its potentialities that is to use it for the prediction of the controlled element gain coefficient in the single loop compensatory tracking task. This model was modified again for evaluating the influence of feel system parameters on pilot-aircraft system characteristics and for selection of these parameters. The main modifications are the following:

- the separation of the limb-manipulator dynamics in two elements: dynamics of limb-muscle system and feel system dynamics;
- the introduction of additional noise n_c, which might be considered as the noise associated with perception of force applied by the pilot to the inceptor. The spectral density of this noise is $S_{n_c n_c} = 0.003\pi\sigma_c^2$;
- the extension of the cost function. The additional term $\beta\sigma_F^2$ was added to reflect the influence of the spring stiffness on pilot workload mentioned above and closed-loop system characteristics:

$$I = \sigma_e^2 + \alpha\sigma_c^2 + \beta\sigma_F^2 .$$

The structural pilot model is shown on fig. 10.

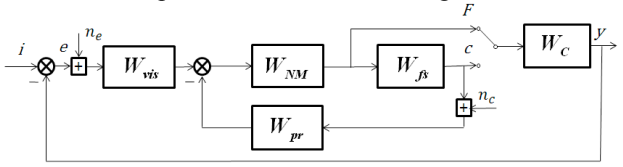

Fig. 10. The structural pilot model

Here W_{fs} – the feel system dynamics (see eq. 1);

$W_{nm} = \frac{1}{T_{N*}s+1} \cdot \frac{e^{-\tau_N s}}{T_N^2 s^2 + 2T_N\xi_N s + 1}$ – the limb muscle system dynamics;

$W_{vis} = \frac{K_L(T_L s+1)}{T_I s+1}e^{-\tau s}$ – pilot error compensation dynamic;

$W_{pr} = \frac{K_n s^2}{T_n^2 s^2 + 2T_n s + 1}$ – proprioceptive feedback;

n_e – perception noise. Its spectral density

$$S_{n_e n_e} = K_{n_e}\pi\frac{\sigma_e^2 + \sigma_{\dot e}^2 T_L^2}{1 + T_L^2\omega^2},\ K_{n_e}=0.01. \qquad [6]$$

The minimization of the cost function allowed to define the parameters T_L, K_L, T_n, K_n (see the fig. 10). The other parameters of the model were constant and equal to $T_N^* = 0.02$ sec, $T_N = 0.1$ sec, $T_I = 0.01$ sec, $\xi_N^* = 1.2$, $\tau = 0.2$ sec, $\tau_N = 0.08$ sec. The weighting coefficient β was accepted 0.001.

The procedure for the minimization of the cost function assumes the calculation of variance $\sigma_e^2, \sigma_{\dot e}^2, \sigma_c^2$ from the following equations:

$$\begin{cases} A_1\sigma_e^2 + B_1\sigma_{\dot e}^2 + C_1\sigma_c^2 = \sigma_{e_i}^2 \\ A_2\sigma_e^2 + B_2\sigma_{\dot e}^2 + C_2\sigma_c^2 = \sigma_{\dot e_i}^2 \\ A_3\sigma_e^2 + B_3\sigma_{\dot e}^2 + C_3\sigma_c^2 = \sigma_{c_i}^2 \end{cases}.$$

Here symbols $\dot e$ and $\dot e_i$ are derivatives of error. The component $\dot e_i$ is correlated with the input signal. The signal c is the displacement signal and c_i is its part which is correlated with the input signal.

The coefficients A_i, B_i and C_i are defined by the corresponding closed loop transfer function, for example:

$$\begin{cases} A_1 = 1 - \frac{K_{n_e}}{\pi}\int_0^\infty \left|\frac{W_P W_C}{1+W_P W_C}\right|^2 \frac{d\omega}{1+T_L^2\omega^2} \\ A_2 = -\frac{K_{n_e}}{\pi}\int_0^\infty \left|\frac{W_P W_C}{1+W_P W_C}\right|^2 \frac{\omega^2}{1+T_L^2\omega^2} d\omega \\ A_3 = -\frac{K_{n_e}}{\pi}\int_0^\infty \left|\frac{W_P}{1+W_P W_C}\right|^2 \frac{d\omega}{1+T_L^2\omega^2} \end{cases}.$$

For FCS inceptor type $W_P = W_{vis}\frac{W_{NM}}{1+W_{NM}W_{pr}W_{fs}}$

For DCS inceptor type $W_P = W_{vis}\frac{W_{NM}W_{fs}}{1+W_{NM}W_{pr}W_{fs}}$

With help of the modified structural model the influence of stiffness and type of inceptors (FSC or DSC) was investigated. The results of the modeling demonstrated the same influence of the investigated parameters on pilot-vehicle system characteristics as in experimental investigations and a good agreement between the results of experimental and mathematical modeling (fig. 11-13).

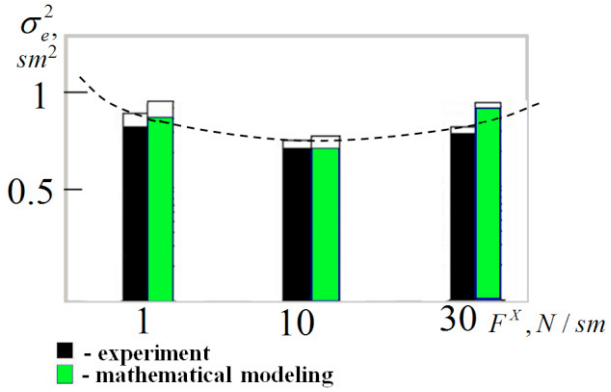

Fig. 11.The influence of the stiffness

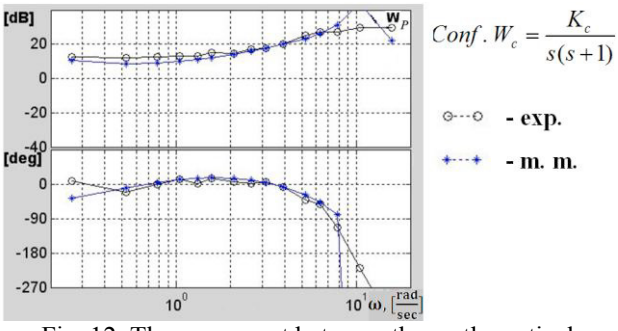

Fig. 12. The agreement between the mathematical modeling and experimental results

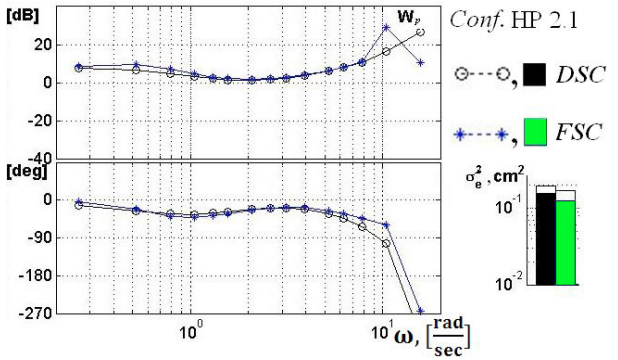

Fig. 13. The influence of the type of inceptor (mathematical modeling)

CONCLUSION

The considerable decrease of the pilot phase delay (up to 90 – 102 deg) and variance of error (up to 30÷40%) were exposed in pitch and lateral control tracking tasks with the force sensing control in comparison with displacement sensing control type of inceptor. This effect increases with the decrease of the spring stiffness for the central stick as well as for the side stick. The dependence of variance of error as the function of the inceptor's spring stiffness F^x demonstrated the existence of the minimum located at the moderate value of F^x. The use of the side stick requiring pilot's rotation of his hand in lateral channel leads to increase in time delay up to 0.15 sec in comparison with translational movements of the side stick accompanying the pilot's control actions in the lateral channel. The revision of the pilot structural model allowed to evaluate the influence of some feel system parameters on the pilot-aircraft system characteristics and provides good agreement with the results of experimental investigations.

REFERENCES

1. R.E. Magdaleno, D.T. McRuer, "*Effects of Manipulator Restraints on Human Operator Performance"*, AFFDL-TR-66-72, Dec. 1966.
2. D.E. Johnston, D.T. McRuer, "*Investigation of Interactions Between Limb-Manipulator Dynamics and Effective Vehicle Roll Control Characteristics"*, NASA CR-3983, May 1986.
3. David G. Mitchell, Bimal L. Aponso, and David H. Klyde, "*Effects of Cockpit Lateral Stick Characteristics on Handling Qualities and Pilot Dynamics"*, NASA CR-4443, Jun. 1992.
4. Deniz Yilmaz, Michael Jump, Lu Linghai, Michael Jones, "*Aircraft and Rotorcraft Pilot Couplings – Tools and Techniques for Alleviation and Detection"*, ACPO-GA-2010-266073 Deliverable No. D2.3 State-of-the-art pilot model for RPC prediction report, Apr. 2011.
5. Larisa E. Zaychik, Kirill N. Grinev, Yury P. Yashin, Sergey A. Sorokin, "*Effect of Feel System Characteristics on Pilot Model Parameters"*, Proceedings of the 1st IFAC Conference on Cyber-Physical & Human-System, Florianopolis, Brasil, Dec. 2016.
6. A.V. Efremov, A.V. Ogloblin, A.N. Predtechensky, V.V. Rodchenko., "*Pilot as a dynamic system*", Moscow: Mashinostroyeniye, 1992, 336 pp.
7. David H. Klyde and Duane McRuer, "*Smart-Cue and Smart-Gain Concepts Development to Alleviate Loss of Control"*, Journal of Guidance, Control, and Dynamics Vol. 32, No. 5, Sep.-Oct. 2009.
8. David H. Klyde and Chi-Ying Liang, "*Approach and Landing Flight Evaluation of Smart Cue and Smart-Gain Concepts"*, Journal of Guidance, Control, and Dynamics Vol. 32, No. 4, Jul.-Aug. 2009.
9. A.V. Efremov, M.S. Tjaglik, U.V. Tiumentzev, Tan Wenqian, *"Pilot behavior modeling and its application to manual control tasks"*, IFAC-PapersOnLine, 49(32), c. 159-164, 2016
10. E. Bjorkman, "*Flight test evaluation of to predict longitudinal pilot-indused oscillation"*, Ph.D. Thesis, 1996
11. R. Hess, *"Structural model of the adaptive human pilot"*, J. of Guidance and Control, Vol. 3, № 5, 1979, pp. 416-423.